Synthesis and Antiviral Activity of Ethidium−Arginine Conjugates Directed Against the TAR RNA of HIV-1

Valérie Peytou,[†] Roger Condom,*[,†] Nadia Patino,[†] Roger Guedj,[†] Anne-Marie Aubertin,[‡] Nathalie Gelus,[§] Christian Bailly,[§] Raphaël Terreux,[||] and Daniel Cabrol-Bass[||]

Laboratoire de Chimie Bioorganique, CNRS ESA 6001, Université de Nice Sophia-Antipolis, F-06108 Nice Cedex 2, France, INSERM-U74, Université Louis Pasteur, Institut de Virologie, 3 rue Koeberlé, F-67000 Strasbourg, France, Laboratoire de Pharmacologie Antitumorale du Centre Oscar Lambret, INSERM-U524, IRCL, Place de Verdun, F-59045 Lille, France, and LARTIC, Université de Nice Sophia-Antipolis, F-06108 Nice Cedex 2, France

Received December 23, 1998

The regulatory protein Tat is essential for viral gene expression and replication of the human immunodeficiency virus type 1 (HIV-1). Tat transactivates the HIV-1 long terminal repeat (LTR) via its binding to the transactivation responsive element (TAR) and increases the viral transcription. Studies have shown that the binding of arginine and arginine derivatives induces a conformational change of the TAR RNA at the Tat-binding site. The unpaired A17 residue delimits a small cavity which constitutes a receptor site for small molecules, especially for ethidium bromide. These binding characteristics have prompted us to design a series of ethidium−arginine conjugates capable of interacting with the TAR RNA. Here we report the synthesis of six ethidium derivatives equipped with arginine side chains. These molecules were biologically evaluated, and two compounds (**17** and **20**) exhibited in vitro anti-HIV-1 activity at micromolar concentration, without toxicity (up to 100 μM concentration). Melting temperature studies indicated that the most active molecule (**20**) bound strongly to TAR in vitro. RNase protection experiments agreed with the molecular modeling studies which suggested that the ethidium moiety of **20** was inserted next to the A17 residue while the arginine side chain occupied the pyrimidine bulge.

Introduction

Acquired immune deficiency syndrome (AIDS) is the final stage resulting from a gradual but accelerating decline in immune competence characterized by immune dysfunction and depletion of CD4 T helper T-cells. The causative agent of AIDS is the human immunodeficiency virus type 1 (HIV-1), discovered in 1983.[1] The gene expression is regulated by a number of virus-encoded proteins, including the transactivator of transcription (Tat) protein which plays a determinant role in virus replication.[2] Tat is responsible for high levels of expression from the viral long terminal repeat (LTR) promoter involving the interaction of Tat with the viral RNA at a specific region, called transactivation responsive element (TAR).[3,4] Tat also acts by increasing the initiation level of the LTR transcription.[5] The goal of HIV therapeutics is to attempt to stop or at least to slow HIV disease progression. The TAR RNA represents an attractive therapeutic target for the design of antiviral drugs.

HIV-1 Tat is an 86-amino acid protein produced from a doubly spliced mRNA formed by joining an exon preceding the *env* gene with the second exon within *env*. Mutational and NMR analyses have revealed different structural and functional domains.[6,7] One of the domains, the basic region (residues 48−57: Gly Arg Lys Lys Arg Arg Gln Arg Arg Arg), is involved in TAR RNA binding.[8] While lysine residues contribute to electrostatic interactions, the arginine at position 52 is the only sequence contact mediating the complex formation between Tat and TAR.[9] HIV-1 TAR is a sequence of 59 nucleotides located downstream from the transcription initiation site in the LTR.[10,11] It forms a hairpin stem−loop structure consisting of base-pair interactions between nucleotides +1 to +59. It contains a 6-nucleotide loop (residues 30−35) and a 3-nucleotide pyrimidine bulge (residues 23−25) (Chart 1).[12−14] That the bulge is essential for high affinity and specific binding of the Tat protein is evidenced by a number of studies.

First, dynamic molecular modeling studies have shown a conformational change of TAR between the free and the Tat-bound form of the RNA.[15] Studies suggested that U23, C24, and U25 are stacked on A22 in the absence of Tat and that the arrangement of the 3-nucleotide bulge is disrupted in the presence of Tat or a single arginine: U23 moves in direct proximity to G26, and the two other nucleotides become unstacked.[16−18] Tat binds to TAR precisely in the region of the bulge UCU of TAR via an arginine residue and recognizes both the identity of adjacent Watson−Crick base pairs and the positions of surrounding phosphate groups.[19−22] On the basis of NMR spectra of the truncated TAR sequence associated with derivatives of arginine or derivatives of Tat, a structural model of the complex was proposed.[17,23−25] This model has shown that residues U23, A27, and G26 interact with the guanidinium group of arginine 52. Thus, a large part around the bulge is critical for formation of the Tat−TAR complex. Second, it is im-

* Corresponding author: Prof. Roger Condom. Tel: (+33) (0)4 92 07 61 52. Fax: (+33) (0)4 92 07 61 51. E-mail: condom@unice.fr.
[†] Laboratoire de Chimie Bioorganique.
[‡] Institut de Virologie.
[§] Laboratoire de Pharmacologie Antitumorale.
[||] LARTIC.

10.1021/jm980728e CCC: $18.00
Published on Web 09/21/1999

Chart 1. Structure of the TAR RNA of HIV-1

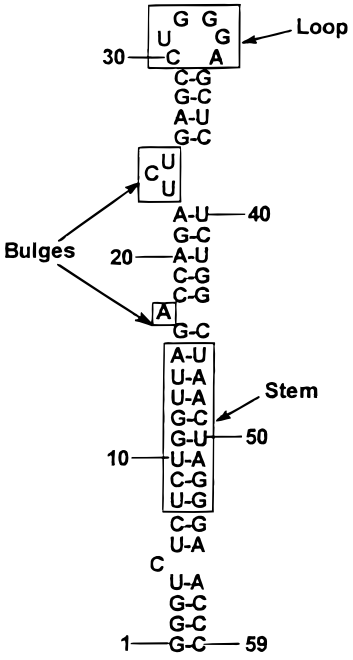

portant to note that a single arginine residue in solution binds to the bulge of TAR with millimolar affinity.[26] Third, a number of RNA-interacting compounds including groove binders, classical and threading intercalators, unfused aromatic intercalators, and agents with mixed binding modes have been identified.[27] Some classical intercalating agents, such as ethidium bromide, were found to bind more tightly to RNA than to DNA.[27] With DNA, ethidium exhibits a slight preference for binding to pyrimidine(3′-5′)purine sites and particularly to CpG steps.[28−31] With different RNA hairpin segments, ethidium also binds preferentially to CpG sites proximal to a bulge.[32,33] More recent studies have revealed that, upon binding to TAR, ethidium intercalates near the unpaired A17 residue.[34,35] Molecular studies have shown that the amino groups at the 3 and 8 positions of ethidium are critical components in ethidium interactions with nucleic acids and that the geometry of the phenanthridine ring system is nearly ideal for maximizing favorable contacts with the nucleic acid bases that form the top and the bottom of the intercalation site.[36] Therefore, the development of agents which may interfere with the protein−RNA complex formation is a potential strategy for controlling the proliferation of HIV.[37−49]

The capacity of ethidium to form stable complexes with RNA including TAR, on the one hand, and the fact that arginine and arginine derivatives bind to the pyrimidine bulge of TAR, on the other hand, prompted us to design bifunctional molecules capable of binding to both binding sites of TAR. For this purpose, we synthesized a series of molecules containing: (i) an arginine residue which would bind near the U23-C24-U25 bulge, (ii) an ethidium moiety which would intercalate between the base pairs C18-G44 and C19-G43, close to the A17 bulge, and (iii) a spacer arm connecting the two RNA-binding parts of the molecule (Chart 2). Spacer arms of variable length were prepared in order to determine the optimal distance needed to allow the two parts of the molecules to interact with TAR. The

Chart 2. Intercalation of the Potential Inhibitors Directed Against the TAR RNA of HIV-1

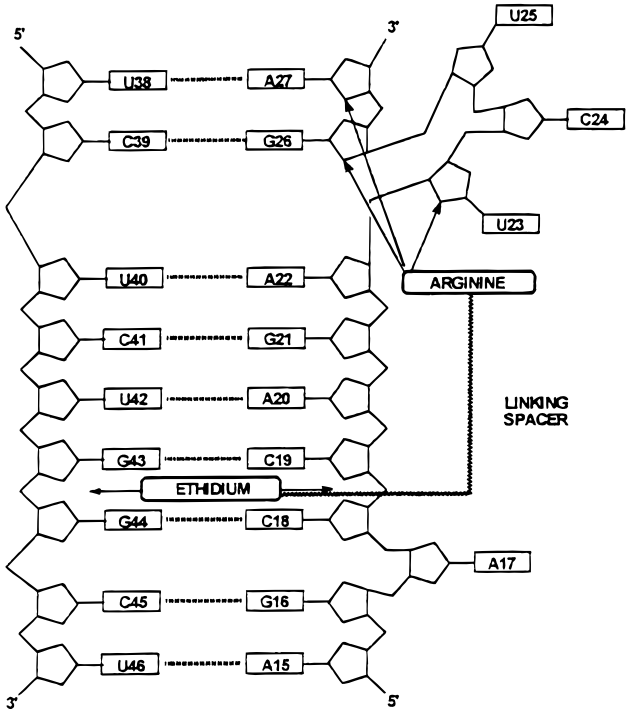

arginine residue was attached to the 3′ (*meta*) position of the ethidium chromophore. Previous studies have shown that substitutions at the *meta* position cause minimal interference with the intercalation binding mode.[50]

The synthesis and the anti-HIV-1 activity of a series of six molecules against different cell lines in vitro are presented here. Two of them (**17** and **20**) exhibited in vitro anti-HIV-1 activity at micromolar concentration without toxicity (up to 100 μM concentration). The binding to TAR of the most active compound **20** was investigated using melting temperature and RNase footprinting experiments, and the drug−TAR RNA complex formation was also studied by molecular modeling.

Chemistry

The synthesis of the ethidium derivatives was carried out in three principal steps. First, a modified ethidium molecule (**8**) was synthesized. We introduced a carboxyl function to the *meta* position of the 6-phenyl group for use in anchoring an arginine-terminated chain via an amide linkage. Second, we synthesized a series of molecules (**9**−**11**) containing an amino group and an arginine residue separated by a spacer. Third, coupling of these two key molecules followed by deprotection of the guanidinium ion yielded the final compounds **15**−**20** (Scheme 1).

Carboxyethidium derivative **8** was synthesized using previously described procedures[50−53] with some modifications. 2-Aminobiphenyl (**1**) was acylated with 3-cyanobenzoyl chloride (**2**) in chlorobenzene to give amide **3**, which was then cyclized to give phenanthridine **4** by refluxing with phosphoryl chloride in nitrobenzene. The use of tin(IV) chloride to catalyze the reaction provided **4** in good yield.[54] Hydrolysis of the nitrile of the phenanthridine **4** in 75% H_2SO_4 gave carboxylic acid

Scheme 1. Route Leading to Potential Inhibitors

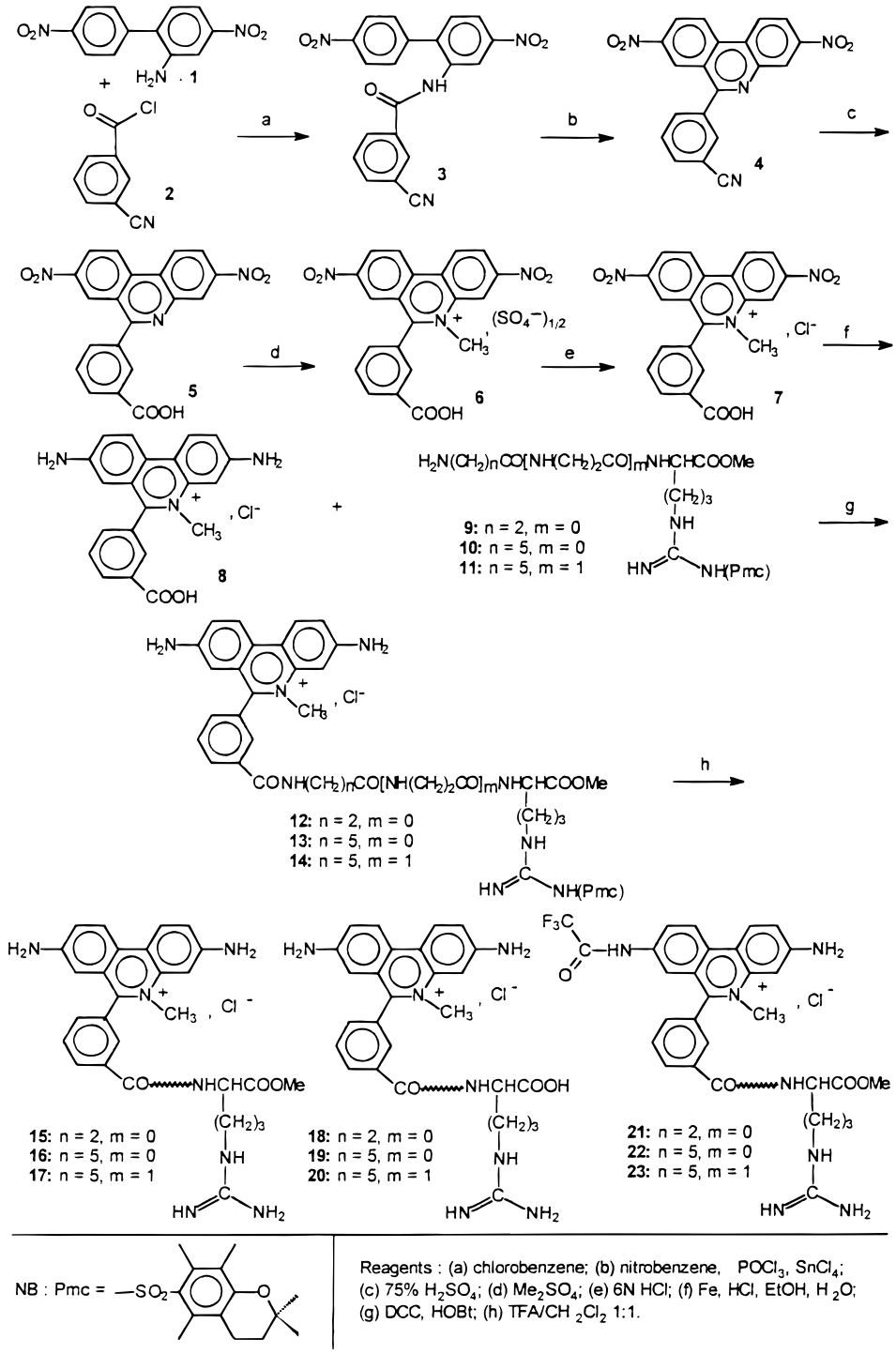

derivative **5**. Quaternization of phenanthridine **5** was carried out using dimethyl sulfate, which also methylated the carboxyl group to lead to methyl ester **6**, in the form of a very hygroscopic oil. **6** was refluxed in a 6 N HCl aqueous solution and gave the carboxylic acid derivative **7**, in chloride ion form. Finally, **7** was reduced using iron powder in the presence of 1 N HCl in water−ethanol mixture, yielding the key ethidium chloride derivative **8**. Purification following the reduction step was quite difficult and required repeated runs through an Amberlite XAD-2 resin column.

Compounds **9**−**11** were obtained in three steps (Scheme 2). *N*-(Benzyloxycarbonyl)-*β*-alanine was activated using DCC/HOSu and coupled in situ with the H-Arg(Pmc)OH to lead to acid **24**. Then, the carboxyl function was methylated by adding methyl iodide and cesium carbonate to give methyl ester **25**. Deprotection of the primary amine of **25** was realized using catalytic hydrogenation in the presence of 10% Pd/C to produce the first arginine-terminated chain **9**, for linking with the carboxyethidium **8**. The second arginine-terminated chain **10** was prepared following the same route starting from *N*-(benzyloxycarbonyl)caproic acid. Intermediate compounds **26** and **27** were isolated at each step of the synthesis. Finally, coupling of *N*-(benzyloxycarbonyl)-caproic acid with **9** gave methyl ester **28** which was

Scheme 2. Route Leading to the Arginine-Linking Chains

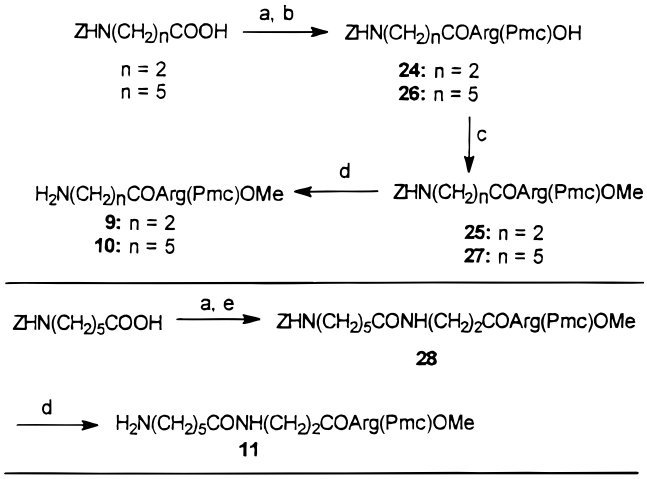

Reagents : (a) DCC, HOSu; (b) HArg(Pmc)OH; (c) MeI, Cs_2CO_3; (d) H_2 , 10% Pd/C, MeOH; (e) $H_2N(CH_2)_2COArg(Pmc)OMe$ **9.**

catalytically hydrogenated to led to the third arginine-terminated chain **11**.

Next, the modified ethidium chloride **8** was joined to each of the three arginine-linking chains via amide linkages to yield, after further reactions, three target inhibitor molecules containing two binding sites (**15**−**17**). First, protected compounds **12**−**14** were prepared by condensation of the carboxyl group of the modified ethidium chloride **8** and the primary amino groups of each of the three different arginine-terminated chains **9**−**11**. The DCC/HOBt coupling method was used to obtain compounds **12**−**14** in good yield (78−89%). Then, the N^G-2,2,5,7,8-pentamethylchroman-6-sulfonyl (Pmc) groups (protecting the guanidine side-chain function of arginine) were removed using trifluoroacetic acid (TFA) or 50% TFA in dichloromethane (DC) at room temperature.[56,57] Although the Pmc groups were cline removed, the TFA/DC (1:1) reagent resulted in partial solvolysis of the methyl carboxylate groups. Thus, in addition to obtaining the three target inhibitor molecules **15**−**17**, the corresponding fully deprotected derivatives **18**−**20** were also obtained. In addition to these compounds, side products with a trifluoroacetamido group at the 7 position of phenanthridine appeared (compounds **21**−**23**). HPLC was used to monitor the deprotection steps to minimize the yield of side products. The three products obtained during each deprotection reaction were separated by semipreparative HPLC. Yields for the deprotection reactions are given in Table 1. Molecules **15**−**20** were characterized using mass spectrometry (electrospray method (ESI)), proton and carbon NMR data, and infrared spectrometry. Purity of all compounds was determined by HPLC.

Results and Discussion

In Vitro Biological Evaluation. The anti-HIV-1 activity of compounds **15**−**20** and ethidium **8** (used as a reference) was evaluated in infected CEM-SS, MT4, and PBMC cells. Arginine and ethidium compounds were included in the biological evaluation testing. As arginine was devoid of activity, we have chosen to keep ethidium as a reference. So, we have shown that an increased viral inhibition was measured with some ethidium−arginine conjugates compared with an already "active" compound. The results are given in Table 2.

Table 1. Yields of the Deprotection Step Leading to Compounds **15**−**23**

chain length	ester form	acid form	side product
$n = 2$, $m = 0$	**15**, 40%	**18**, 21%	**21**, 25%
$n = 5$, $m = 0$	**16**, 37%	**19**, 15%	**22**, 28%
$n = 5$, $m = 1$	**17**, 39%	**20**, 23%	**23**, 24%

Compounds **15**, **16**, **18**, and **19**, which all contain a short spacer [$NH(CH_2)_2CO$ for **15** and **18**, $NH(CH_2)_5CO$ for **16** and **19**], were devoid of anti-HIV-1 activity at concentrations up to 100 μM (or at nontoxic concentrations), in infected CEM-SS, MT4, and PBMC cell lines. In sharp contrast, under the same conditions, compounds **17** and **20** containing the longest spacer [$NH(CH_2)_5CONH(CH_2)_2CO$] reduced viral multiplication by 50% at a micromolar concentration without apparent cellular toxicity up to 100 μM concentration, on cultures of CEM-SS and PBMC cells acutely infected by HIV-1. However, on cultures of MT4 cells the anti-HIV-1 activity of **17** was strongly diminished. On the basis of the promising biological data obtained with **20**, the most active conjugate in the series, the interaction of this drug with TAR was investigated using complementary biochemical methods as well as molecular modeling.

Experiments were performed by Dr. Pierre Charneau, from Institut Pasteur, France, concerning the intercalation of compounds **17** and **20** with TAR. They have shown that, first, these compounds interact with TAR at the second stage of the cellular infection and, second, they reach the inside of the cells.

Dynamic Molecular Modeling Studies. A molecular modeling study was conducted to support the design of this inhibitory family. The three-dimensional structures of (i) Tat protein−TAR RNA complex, (ii) free TAR RNA, and (iii) TAR RNA with an arginine residue were used. The coordinates were obtained from the Protein Data Bank.

The Tat protein−TAR RNA interaction site is located between the C19 and A22 nucleotides, in the major groove of the TAR RNA. Analysis of the structure of the TAR RNA−arginine residue complex showed that arginine interacted with the bases of the bulge region. This interaction induced rotations of these bases which had several effects. The first one was to fold the TAR RNA structure, and the second one allowed the interaction of arginine with the C29 and G36 bases. This new interaction site is located deeply in the structure of TAR RNA. This latest position obtained by molecular simulation was in accordance with NMR data. Moreover, analysis of the TAR RNA−ethidium **8** complex confirmed that ethidium **8** could insert between two pairs of RNA nucleotides and that the most energetically favorable intercalation was between GC and CG base pairs. TAR RNA has two GC and CG base-pair sites. The first one, G28-C37 and C29-G36, is located in the high region of TAR, but this part of the structure is deformed and obstructed by the free loop. Therefore, ethidium intercalation was not possible at this site. Differently, the second one, G43-C19 and G44-C18, is located in a pocket formed by the major groove and extended by the A17 externalized nucleotide.

Table 2. Anti-HIV-1 Activity of Compounds **15**−**20** (ethidium **8** as a reference) on Infected and Uninfected CEM-SS, MT4, and PBMC Cell Lines[a]

	CEM-SS		MT4		PBMC	
evaluated molecules	IC_{50}50 (μM)	CC_{50} (μM)	IC_{50} (μM)	CC_{50} (μM)	IC_{50} (μM)	CC_{50} (μM)
8, Eth-COOH (ref)	95	>100	>100	42	20	44
15, Eth ($n = 2$, $m = 0$), ArgOMe	83	85	>100	21	78	47
16, Eth ($n = 5$, $m = 0$), ArgOMe	>100	>100	>100	60	89	>100
17, Eth ($n = 5$, $m = 1$), ArgOMe	4.6	>100	>100 (38%)	>100 (45%)	8.7	>100
18, Eth ($n = 2$, $m = 0$), ArgOH	>100	>100	>100	47	73	>100
19, Eth ($n = 5$, $m = 0$), ArgOH	>100	>100	>100	59	>100 (40%)	>100
20, Eth ($n = 5$, $m = 1$), ArgOH	2.4	>100	11	>100	2.5	>100

[a] When the inhibition did not reach 50%, the measured value is indicated in parentheses.

Interaction between TAR RNA and compounds **15**−**20** was then modeled. In the first phase, the arginine residue drives the molecule to the TAR RNA−arginine interaction site. Arginine interacted with the bulge bases and induced a conformational change of the bulge. The structure of TAR RNA folded up and the arginine residue interacted with C29 and G36. At this stage of the simulation, the tested molecule was roughly in a linear conformation. In the second phase, the compound folded up and the ethidium moiety interacted with the RNA backbone. In the third phase, the ethidium part slipped on the RNA ribbon and the molecule was roughly parallel to the major groove. Analysis of conformers resulting from dynamic simulations in aqueous phase showed that the major groove was wide enough to accommodate the linking spacer insertion. Energetic and geometric studies of the complex with the linking spacer in the major groove showed that there was no close contact; on the contrary, heteroatoms of the linking spacer created stabilizing interactions with the RNA ribbon. These interactions contributed to locking the major groove. At this stage, the length of the linking spacer was critical because if this one was too short, the ethidium moiety could not reach the intercalation site. Different simulations showed that the linking spacer of molecules **15**, **16**, **18**, and **19** was too short for ethidium intercalation, while molecules **17** and **20** had the optimal linking spacer length. Figure 1 shows the final complex between the molecule **20** and the TAR RNA as obtained from the insertion mechanism hypothesis. Ethidium deformation was consistent with intercalation simulations performed with a 4-base-pair RNA duplex.[57]

Melting Temperature Studies. We compared the ability of ethidium **8** and compound **20** to alter the thermal denaturation profile of TAR RNA. Representative melting curves for the free RNA and its complexes with the two drugs are shown in Figure 2.

The helix-to-coil transition occurs at about 54 °C in the absence of drugs. The T_m is shifted to higher temperature with both compounds but the extent of stabilization is markedly different. For a drug/RNA ratio > 0.1, larger ΔT_m values (T_m complex − T_m RNA) were measured with drug **20** and then with ethidium **8**. For example, at a drug/TAR ratio of 0.4, ΔT_m values of 11.5 and 7.5 °C were determined with **20** and **8**, respectively. The data strongly suggest that the presence of the arginine side chain increases significantly the stability of the drug−RNA complex. In other words, the cationic tail seems to play the expected role, reinforcing the interaction with the RNA target.

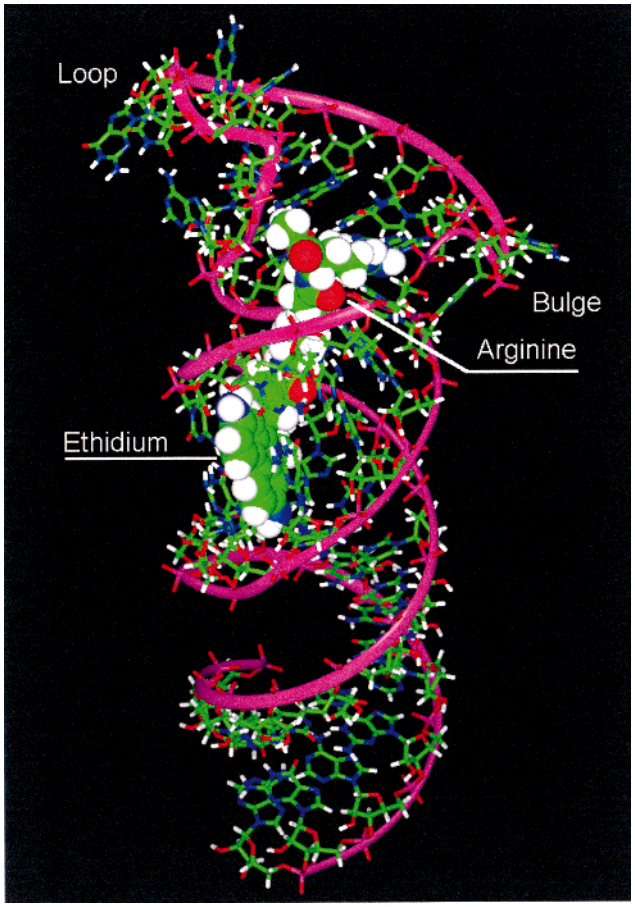

Figure 1. Molecular model of interaction between compound **20** and the TAR RNA of HIV-1. The arginine part is indicated in blue, the linker in yellow, and the ethidium moiety in red. The TAR RNA ribbon is represented as a large pink line.

RNase Protection Experiments.[58] The location of the drug binding site on the TAR RNA was investigated by RNase footprinting using three complementary endonucleases: (i) RNase A which preferentially cuts the single-stranded bulge and loop sequences of TAR rather than the two double-stranded stem regions of the RNA, (ii) RNase T1 which cuts selectively at GpN in single-stranded regions, and (iii) RNase V1 which cleaves RNA predominantly at double-stranded regions. Typical cleavage patterns obtained with TAR cut by the three enzymes in the absence and presence of **20** at concentrations ranging from 0.1 to 2 μM are shown in Figure 3. The alteration of the cleavage profiles are indicated together with their locations on the TAR sequence.

The sites where the enzyme cleavage is modified in the presence of the drug can be divided into two groups: (1) the modification around the A17 unpaired

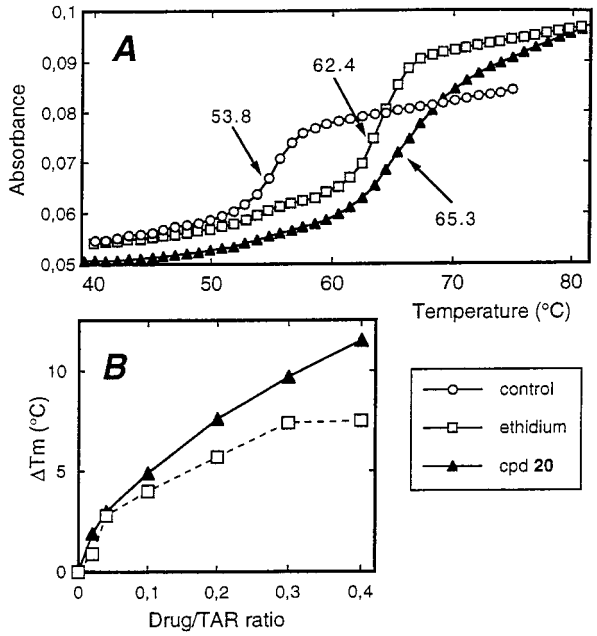

Figure 2. (A) Thermal denaturation curves for TAR in the absence and presence of ethidium **8** and compound **20** at a drug/RNA ratio of 0.4. The indicated T_m values (°C) were obtained from first-derivative plots. (B) Variation of ΔT_m as a function of the drug/RNA ratio.

residue and (2) the protected cleavage sites at or near the pyrimidine bulge. The experiments with RNase T1 show that the drug-induced reduction in cleavage intensity at G44 is accompanied by an enhanced cutting at U46. The extents of enhanced cleavage and protection are proportional to the drug concentration. In the same region, cleavage at A20 by RNase V1 is markedly increased when the drug is bound. The RNase A cleavage at the UC site opposite the pyrimidine bulge is reduced in the presence of **20**. A drug-induced cleavage inhibition can also be detected at A27 and G36 with RNases V1 and T1, respectively. The strong cleavage at the loop by RNase T1 remains unaffected in the presence of the drug. These experiments suggest that the small A bulge around position 17 and/or the upper pyrimidine Tat bulge around position 40 can serve as a binding site for the drug. Although we cannot identify the exact position of the drug-bound molecules, it is gratifying that the footprinting experiments are in agreement with the modeling data presented above. The model for which the ethidium moiety is inserted at the dinucleotide step G43pG44·C18pC19 and the arginine extends into the pyrimidine bulge is fully consistent with the experimental probing experiments. The reduction in cleavage intensity at G44 seen with RNase T1 may reflect the intercalation of the ethidium chromophore, whereas the cleavage inhibition at the UC site facing the bulge would account for the insertion of the arginine moiety into the major groove cavity at the Tat binding site.

Conclusion

In this study, we have shown that rationally designed ethidium−arginine conjugates could act as efficient anti-HIV-1 agents providing that the linker chain between the two RNA-binding entities was sufficiently long. For the most active molecule in the series (**20**), the distance between the $^{+}N\text{-}CH_3$ of the ethidium moiety and the guanidinium cationic end of arginine is about 19 Å. Apparently, this much distance is required for the drug to bind at both RNA-binding sites. Analogues of **20** are now being synthesized.

Experimental Section

General. Reactions were carried out under a nitrogen atmosphere, unless otherwise indicated. All solvents were

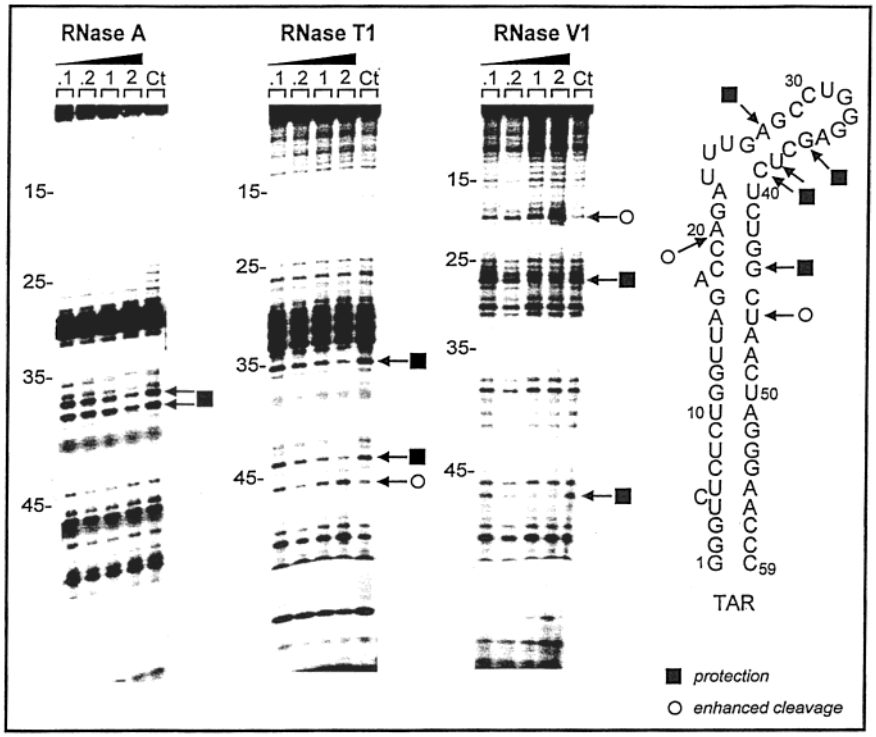

Figure 3. RNase footprinting of compound **20** on TAR. The concentration (μM) of the drug is shown at the top of the appropriate gel lanes. Control tracks labeled "Ct" contained no drug. The sites of cleavage protection and enhancement are indicated on the gels and are reported on the sequence of TAR.

distilled and dried before use, using standard procedures. Thin-layer chromatography (TLC) was run on precoated silica gel plates (Merck 60F 254). Chromatography was carried out on columns packed with silica gel (Merck 60, 230−400 mesh) or on Amberlite XAD-2 resin (20−60 mesh). Melting points were determined using a Büchi capillary instrument and are uncorrected. Nuclear magnetic resonance (NMR) spectra were recorded on a Bruker AC 200 instrument, at 200 MHz. Mass spectra were recorded by direct injection on a INCOS 500E Finnigan MAT spectrometer (chemical ionization or electronic impact, at 70 eV) or a TSQ 7000 Finnigan MAT spectrometer (positive electrospray), via an atmospheric pressure ionization source. Infrared spectra were recorded on a Bruker IFS 45 spectrometer (B) or on a Perkin Elmer Pargon 1000 FT-IR spectrometer (PE). Samples were prepared in KBr disks. Microanalyses were performed in the Vernaison-France Analyses Laboratory (CNRS). HPLC analyses and purifications were performed on a Merck L6200 (M) or on a Hewlett Packard Series 1100 (HP) equipped with UV detectors (at 280 nm), or on a Waters 600 (W) equipped with a diode array detector, using a Lichrospher 100 RP-18 column as support.

1-(3-Cyanobenzamido)-3,8-dinitrobiphenyl (3). 1-Amino-3,8-dinitrobiphenyl (**1**) (5 g, 19.66 mmol) and *m*-benzoyl chloride (**2**) (3.74 g, 22.61 mmol) were refluxed in chlorobenzene (50 mL) for 2 h. After cooling, the reaction mixture was concentrated under reduced pressure and the residue was triturated with chloroforme/diethyl ether/hexane to obtain a white precipitate. After filtration, the product was recrystallized from glacial acetic acid to give pure **3** (91% yield): TLC (Hex/AcOEt, 1:1) R_f = 0.46; mp = 221−223 °C; ^{1}H NMR (DMSO-d_6) δ 10.65 (1H, bs, NH), 8.48 (1H, d, H-1, J = 2.3 Hz), 8.30 (2H, d, H-5 and H-6, J = 8.8 Hz), 8.27 (1H, bs, H-4′), 8.25 (1H, dd, H-2, J = 8.5 Hz, J = 2.3 Hz), 8.09 (1H, d, H-3′, J = 8.4 Hz), 8.05 (1H, d, H-1′, J = 8.4 Hz), 7.81 (2H, d, H-4 and H-7, J = 8.8 Hz), 7.78 (1H, d, H-3, J = 8.5 Hz), 7.72 (1H, t, H-2′, J = 8.4 Hz); ^{13}C NMR (DMSO-d_6) δ 163 (CO−NH), 147 (C−NO_2), 146 (C−NO_2), 111 (CN); IR (B) 3399 (NH), 2230 (CN), 1688 (CO), 1522 (NO_2), 1345 (NO_2); MS m/z = 389 (M + H^+). Anal. ($C_{20}H_{12}N_4O_5$) Calcd: C 61.84, H 3.12, N 14.43. Found: C 61.82, H 3.03, N 13.87. HPLC (W) 280 nm, elution CH_3CN/H_2O (70:30), t_R = 5.00 min.

9-(3-Cyanophenyl)-2,7-dinitrophenanthridine (4). **3** (6.63 g, 16.20 mmol) and $POCl_3$ (2.08 mL, 22.68 mmol) in nitrobenzene (40 mL) were refluxed for 1 h; then tin chloride (0.38 mL, 3.24 mmol) was added. After 2 h, the solution was cooled and nitrobenzene was removed by distillation. The residue was triturated with boiling anhydrous ethanol (120 mL) for 10 min. After filtration, the solid product was washed again with hot anhydrous ethanol to yield a beige powder **4** (98% yield): TLC (Hex/AcOEt, 7:3) R_f = 0.60; mp = 302−304 °C; ^{1}H NMR (DMSO-d_6) δ 9.38 (1H, d, H-4, J = 8.9 Hz), 9.29 (1H, d, H-3, J = 9.1 Hz), 8.98 (1H, d, H-1, J = 2.3 Hz), 8.95 (1H, dd, H-5, J = 8.9 Hz, J = 2.2 Hz), 8.80 (1H, d, H-6, J = 2.2 Hz), 8.64 (1H, dd, H-2, J = 9.1 Hz, J = 2.3 Hz), 8.40 (1H, bs, H-4′), 8.26 (1H, d, H-3′, J = 7.7 Hz), 8.23 (1H, d, H-1′, J = 7.7 Hz), 7.97 (1H, t, H-2′, J = 7.7 Hz); ^{13}C NMR (DMSO-d_6) δ 149 (C−NO_2), 148 (C−NO_2), 113 (CN); IR (B) 2227 (CN), 1518 (NO_2), 1343 (NO_2); MS m/z = 371 (M + H^+). Anal. ($C_{20}H_{10}N_4O_4$) Calcd: C 64.85, H 2.72, N 15.14. Found: C 64.14, H 2.74, N 15.87. HPLC (W) 280 nm, elution CH_3CN/H_2O (70:30), t_R = 8.08 min.

9-(3-Carboxyphenyl)-2,7-dinitrophenanthridine (5). A solution of **4** (6 g, 16.20 mmol) in 75% H_2SO_4 (25 mL) was heated at 130 °C for 2 h. After cooling, the reaction mixture was poured onto crushed ice, adjusted to pH 8.5 with NH_4OH, and then strongly acidified with concentrated HCl. The precipitate was filtered and washed with water until neutral pH. After drying, compound **5** was obtained as a beige-yellow solid (88% yield): TLC (Hex/AcOEt, 3:7) R_f = 0.30; mp = 271−273 °C; ^{1}H NMR (DMSO-d_6) δ 9.21 (1H, d, H-4, J = 9.1 Hz), 9.12 (1H, d, H-3, J = 9.1 Hz), 8.80 (1H, d, H-1, J = 2.2 Hz), 8.77 (1H, d, H-6, J = 2.1 Hz), 8.70 (1H, dd, H-5, J = 9.1 Hz, J = 2.1 Hz), 8.45 (1H, dd, H-2, J = 9.1 Hz, J = 2.2 Hz), 8.33 (1H, bs, H-4′), 8.19 (1H, d, H-3′, J = 7.5 Hz), 7.79 (1H, d, H-1′, J = 7.5 Hz), 7.63 (1H, t, H-2′, J = 7.5 Hz); ^{13}C NMR (DMSO-d_6) δ 166 (COOH), 149 (C−NO_2), 148 (C−NO_2), 144 (C−COOH); IR (B) 3600−3000 (OH), 1616 (CO), 1515 (NO_2), 1345 (NO_2); MS m/z = 390 (M + H^+). Anal. ($C_{20}H_{11}N_3O_6$·HCl) Calcd: C 56.47, H 2.85, N 9.88. Found: C 56.75, H 2.93, N 9.40. HPLC (W) 280 nm, elution gradient CH_3CN/H_2O (20:80 to 50:50) for 30 min, t_R = 7.84 min.

9-(3-Methoxycarbonylphenyl)-2,7-dinitro-10-methylphenanthridine Hemisulfate (6). A solution of **5** (5.3 g, 13.67 mmol) in dimethyl sulfate (40 mL) was refluxed for 3 h. After cooling, addition of diethyl ether (40 mL) resulted in the formation of a dark yellow resin. The residual yellow solution was filtered and the resin dissolved in hot ethanol and then concentrated under reduced pressure to afford **6** as a dark yellow hygroscopic oil which was used without further purification: TLC (Hex/AcOEt, 3:7) R_f = 0.90; ^{1}H NMR (DMSO-d_6) δ 9.60 (2H, m, H-3 and H-4), 9.43 (1H, bs, H-1), 8.98 (2H, m, H-2 and H-5), 8.52 (1H, bs, H-4′), 8.46 (1H, d, H-3′, J = 7.6 Hz), 8.25 (1H, bs, H-6), 8.19 (1H, d, H-1′, J = 7.6 Hz), 8.07 (1H, t, H-2′, J = 7.6 Hz), 4.50 (3H, s, CH_3-N^+), 3.92 (3H, bs, COOMe).

9-(3-Carboxyphenyl)-2,7-dinitro-10-methylphenanthridine Chloride (7). A mixture of **6** (6.3 g, 13.61 mmol) and 6 N HCl (100 mL) was refluxed for 4 h. After cooling, the reaction mixture was concentrated under reduced pressure to afford a brown material. This solid was dissolved in a minimum volume of water and applied to an Amberlite XAD-2 resin column (300 g) which was then washed with H_2O (4 L). Subsequent elution with 50% aqueous methanol yielded orange fractions which were concentrated and dried under reduced pressure to afford **7** as an orange resin (69% yield): TLC (Hex/AcOEt, 3:7) R_f = 0.65 (yellow); ^{1}H NMR (DMSO-d_6) δ 8.47 (1H, d, H-3, J = 8.9 Hz), 8.44 (1H, d, H-4, J = 7.9 Hz), 8.23 (1H, d, H-2, J = 8.9 Hz), 8.01 (1H, bs, H-4′), 7.91 (1H, d, H-3′, J = 7.5 Hz), 7.79 (1H, d, H-1, J = 2.2 Hz), 7.73 (1H, d, H-5, J = 7.9 Hz), 7.65 (2H, m, H-6 and H-1′), 7.54 (1H, t, H-2′, J = 7.5 Hz), 2.83 (3H, s, CH_3-N^+); ^{13}C NMR (DMSO-d_6) δ 166 (COOH), 149 (C=N^+), 146 (C−NO_2), 145 (C−NO_2), 143 (C−COOH), 51 (CH_3-N^+); IR (PE) 3600−2600 (OH), 1643 (CO), 1515 (NO_2), 1341 (NO_2); MS m/z = 404.0 (M^+); HPLC (W) 280 nm, elution gradient CH_3CN/H_2O (1% TFA) (20:80 to 50:50) for 30 min, t_R = 17.32 min.

9-(3-Carboxyphenyl)-2,7-diamino-10-methylphenanthridine Chloride (8). A solution of **7** (3.7 g, 8.41 mmol) in 1 N HCl was refluxed for 4 h. After cooling to ambient temperature, H_2O (19 mL), ethanol (106 mL), and Fe (4.25 g, 76.53 mmol) were added in the order specified with vigorous stirring and the resulting mixture was refluxed for 4 additional hours. The hot mixture was filtered through Celite, and the filtrate was reduced under reduced pressure. The concentrated solution was then applied to an Amberlite XAD-2 resin column (200 g) which was then washed with H_2O (2 L). Subsequent elution with 50% aqueous methanol yielded red fractions which were concentrated and dried under reduced pressure to afford **8** as a purple powder (55% yield): TLC (Hex/AcOEt, 3:7) R_f = 0.65 (red); mp = 258−260 °C; ^{1}H NMR (DMSO-d_6) δ 8.58 (1H, d, H-3, J = 9.4 Hz), 8.53 (1H, d, H-4, J = 9.2 Hz), 8.18 (1H, d, H-3′, J = 7.5 Hz), 8.02 (1H, bs, H-4′), 7.63 (1H, t, H-2′, J = 7.5 Hz), 7.50 (2H,m, H-5 and H-1′), 7.30 (2H, m, H-1 and H-2), 6.58 (2H, bs, $NH_2\alpha$), 6.35 (1H, d, H-6, J = 2.0 Hz), 5.99 (2H, bs, $NH_2\beta$), 3.94 (3H, s, CH_3-N^+); ^{13}C NMR (DMSO-d_6) δ 167 (COOH), 159 (C=N^+), 150 (C−NH_2), 147 (C−NH_2), 141 (C−COOH), 48 (CH_3-N^+); IR (PE) 3600−2600 (OH + 2NH_2), 1643 (CO); MS m/z = 344.1 (M^+). Anal. ($C_{21}H_{18}N_3O_2Cl$) Calcd: C 66.47, H 4.79, N 11.08. Found: C 66.17, H 4.72, N 10.90. HPLC (W) 288 nm, elution gradient CH_3CN/H_2O (1% TFA) (20:80 to 50:50) for 20 min, t_R = 11.48 min.

***N*-α-(*β*-Alanyl)-*N*-(2,2,5,7,8-pentamethylchroman-6-sulfonyl)arginine Methyl Ester (9).** **25** (100 mg, 0.15 mmol) and 10% Pd/C (16 mg, 0.15 mmol) were placed, at 0 °C, in methanol. The reaction mixture was placed under hydrogen flow for 3 h. After removal of Pd/C through Celite, methanol was removed under reduced pressure and trituration with diethyl ether afforded **9** as white crystals (99% yield). This product was used without further purification: mp = 130−132 °C; ^{1}H NMR (CD_3OD) δ 4.25 (1H, m, CH), 3.55 (3H, s,

OMe), 3.05 (2H, m, CH_2-1), 2.80 (2H, m, CH_2-5), 2.55 (2H, m, CH_2-2), 2.45 (6H, s, $2CH_3$(o)), 2.30 (2H, m, $CH_2\beta$), 2.00 (3H, s, CH_3(m)), 1.75−1.45 (6H, m, CH_2-3, CH_2-4 and $CH_2\alpha$), 1.20 (6H, m, $2CH_3$gem).

***N*-α-(Aminocaproyl)-*N*-(2,2,5,7,8-pentamethylchroman-6-sulfonyl)arginine Methyl Ester (10).** This was prepared from **27** (70 mg, 0.10 mmol) by a method analogous to that for **9**. Compound **10** was collected as white crystals (98% yield). This product was used without further purification: mp = 135−137 °C; ^{1}H NMR ($CDCl_3$) δ 6.80 (2H, m, NH_2a), 6.20 (3H, m, NHc, NHd and NHe), 4.50 (1H, m, CH, m), 3.70 (3H, s, OMe), 3.15 (4H, m, CH_2-1 and CH_2-6), 2.50 (10H, m, CH_2-3, $2CH_3$(o) and $CH_2\beta$), 2.30 (2H, m, $CH_2\alpha$), 2.05 (3H, s, CH_3(m)), 1.60 (4H, m, CH_2-4 and CH_2-5), 1.50 (6H, m, $3CH_2$-2), 1.30 (6H, m, $2CH_3$gem).

***N*-α-[(Aminocaproyl)-β-alanyl]-*N*-(2,2,5,7,8-pentamethylchroman-6-sulfonyl)arginine Methyl Ester (11).** This was prepared from **28** (586 mg, 0.75 mmol) by a method analogous to that for **9**, except the product was crystallized from dichloromethane/diethyl ether. Compound **11** was isolated as white crystals (96% yield). This product was used without further purification: mp = 126−128 °C; ^{1}H NMR ($CDCl_3$) δ 6.80 (2H, m, NH_2a), 6.20 (4H, m, NHc, NHd, NHe and NHf), 4.50 (1H, m, CH), 3.70 (3H, s, OMe), 3.15 (4H, m, CH_2-1 and CH_2-8), 3.05 (2H, m, CH_2-4), 2.50 (12H, m, CH_2-3, CH_2-5, $2CH_3$(o) and $CH_2\beta$), 2.30 (2H, m, $CH_2\alpha$), 2.05 (3H, s, CH_3(m)), 1.60 (4H, m, CH_2-6 and CH_2-7), 1.50 (6H, m, $3CH_2$-2), 1.30 (6H, m, $2CH_3$gem).

9-[3-[[[*N*-(2,2,5,7,8-Pentamethylchroman-6-sulfonyl)arginine methyl ester]-β-alanyl]keto]phenyl]-2,7-diamino-10-methylphenanthridine Chloride (12). 8 (100 mg, 0.26 mmol), 1-hydroxybenzotriazole (35.5 mg, 0.26 mmol), and **9** (276.5 mg, 0.52 mmol) were dissolved in dimethylformamide (DMF), at 0 °C. After 10 min, 1,3-dicyclohexylcarbodiimide (54.3 mg, 0.26 mmol) was added and the reaction mixture was stirred for 18 h. DMF was removed under reduced pressure, and the residue was washed with 5% aqueous NH_4OH solution, then with 1 N HCl aqueous solution, and finally with ethyl acetate. There was a solid product left, which was dissolved in methanol. This organic layer was dried on $MgSO_4$ and then concentrated under reduced pressure. The product was purified by passing through an Amberlite XAD-2 column (50 g) with elution with a 5% methanol in water (500 mL)−100% methanol gradient. Red fractions were concentrated under reduced pressure to give **12** as a purple resin (89% yield). This product was used without further purification: ^{1}H NMR (DMSO-d_6) δ 8.99 (1H, bs, NHa), 8.66 (2H, m, H-3 and H-4), 8.20 (2H, m, H-3′ and H-4′), 7.82 (3H, m, H-1′, H-2′ and H-5), 7.34 (2H, m, H-1 and H-2), 7.20−6.90 (4H, m, NHb, NHc, NHd and NHe), 6.54 (2H, bs, $NH_2\alpha$), 6.35 (1H, s, H-6), 6.04 (2H, bs, $NH_2\beta$), 4.16 (1H, m, CH), 3.99 (3H, s, CH_3 -N^+), 3.50 (5H, m, OMe and CH_2-1), 2.99 (2H, m, CH_2-5), 2.60−2.45 (8H, m, $2CH_3$(o) and CH_2-2), 2.04 (3H, s, CH_3(m)), 1.80−1.15 (14H, m, CH_2-3, CH_2-4, $CH_2\alpha$, $CH_2\beta$ and $2CH_3$gem); IR (PE) 3600−3000 ($2NH_2$+5NH), 1643 (CO), 1627 (2CO), 1112 (COMe); MS *m*/*z* = 851.4 (M^+); HPLC (HP) 288 nm, elution gradient CH_3CN/H_2O (1% TFA) (20:80 to 100:0) for 30 min, t_R = 29.18 min.

9-[3-[[[*N*-(2,2,5,7,8-Pentamethylchroman-6-sulfonyl)arginine methyl ester]aminocaproyl]keto]phenyl]-2,7-diamino-10-methylphenanthridine Chloride (13). This was prepared from **8** (100 mg, 0.26 mmol) and **10** (295 mg, 0.52 mmol) by a method analogous to that for **12** above, and **13** was isolated as a purple resin (78% yield). This product was used without further purification: ^{1}H NMR (DMSO-d_6) δ 8.82 (1H, bs, NHa), 8.64 (2H, m, H-3 and H-4), 8.22 (2H, m, H-3′ and H-4′), 7.83 (3H, m, H-1′, H-2′ and H-5), 7.55−7.15 (6H, m, H-1, H-2, NHb, NHc, NHd and NHe), 7.00 (2H, bs, $NH_2\alpha$), 6.56 (2H, bs, $NH_2\beta$), 6.35 (1H, s, H-6), 4.18 (1H, m, CH), 3.98 (3H, s, CH_3-N^+), 3.58 (3H, s, OMe), 3.16 (2H, m, CH_2-1), 3.00 (2H, m, CH_2-6), 2.60−2.45 (8H, m, $2CH_3$(o) and CH_2-3), 2.12 (2H, m, $CH_2\beta$), 2.02 (3H, s, CH_3(m)), 1.80−1.00 (18H, m, $3CH_2$-2, CH_2-4, CH_2-5, $CH_2\alpha$ and $2CH_3$gem); IR (PE) 3600−3000 ($2NH_2$ + 5NH), 1640 (CO), 1625 (2CO), 1109 (COMe); MS *m*/*z* = 893.5 (M^+); HPLC (HP) 288 nm, elution gradient CH_3CN/H_2O (1‰ TFA) (20:80 to 100:0) for 30 min, t_R = 29.89 min.

9-[3-[[[[*N*-(2,2,5,7,8-Pentamethylchroman-6-sulfonyl)-arginine methyl ester]-β-alanyl]aminocaproyl]keto]phenyl]-2,7-diamino-10-methylphenanthridine Chloride (14). This was prepared from **8** (60 mg, 0.16 mmol) and **11** (205 mg, 0.32 mmol) by a method entirely analogous to that for **12** above, and **14** was isolated as a purple resin (87% yield). This product was used without further purification: ^{1}H NMR (DMSO-d_6) δ 8.82 (1H, bs, NHa), 8.63 (2H, m, H-3 and H-4), 8.25 (2H, m, H-3′ and H-4′), 7.84 (3H, m, H-1′, H-2′ and H-5), 7.67 (1H, bs, NHb), 7.32 (3H, m, H-1, H-2 and NHc), 6.72 (3H, m, NHd, NHe and NHf), 6.48 (2H, bs, $NH_2\alpha$), 6.34 (1H, s, H-6), 6.00 (2H, bs, $NH_2\beta$), 4.16 (1H, m, CH), 3.98 (3H, s, CH_3-N^+), 3.52 (3H, s, OMe), 3.22 (4H, m, CH_2-1 and CH_2-4), 3.01 (2H, m, CH_2-8), 2.60−2.40 (10H, m, $2CH_3$(o), CH_2-5 and $CH_2\beta$), 2.28 (2H, m, CH_2-3), 2.02 (3H, s, CH_3(m)), 1.95−1.15 (18H, m, $3CH_2$-2, CH_2-6, CH_2-7, $CH_2\alpha$ and $2CH_3$gem); IR (PE) 3600−3000 ($2NH_2$ + 6NH), 1642 (CO), 1625 (2CO), 1109 (COMe); MS *m*/*z* = 964.5 (M^+); HPLC (HP) 288 nm, elution gradient CH_3CN/H_2O (1% TFA) (20:80 to 100:0) for 30 min, t_R = 29.45 min.

9-[3-[[(Arginine methyl ester)-β-alanyl]keto]phenyl]-2,7-diamino-10-methylphenanthridine Chloride (15) and 9-[3-[(Arginyl-β-alanyl)keto]phenyl]-2,7-diamino-10-methylphenanthridine Chloride (18). 12 (173 mg, 0.20 mmol) was added to 50% trifluoroacetic acid in dichloromethane (DC) (4 mL). HPLC was used to monitor the process and to stop the reaction as soon as the side product appeared (about 1.5 h 30). The reaction mixture was concentrated under reduced pressure, without heating, then repeatedly dissolved in DC, and concentrated again several times. The product was further purified by reverse-phase semipreparative HPLC (CH_3CN/H_2O (1% TFA) 20:80, gradient 100:0 for 60 min). Three compounds were isolated: the ester **15**, the acid **18**, and the side product **21** in 40%, 21%, and 25% yields, respectively, as purple resins for **15** and **21** and an orange resin for **18**.

Compound 15: ^{1}H NMR (D_2O) δ 8.60 (2H, m, H-3 and H-4), 8.07 (1H, d, H-3′, *J* = 7.6 Hz), 7.65 (4H, m, H-1′, H-2′, H-4′ and H-5), 7.35 (2H, m, H-1 and H-2), 6.72 (1H, s, H-6), 4.25 (1H, m, CH), 4.07 (3H, s, CH_3-N^+), 3.73 (3H, s, OMe), 3.48 (2H, m, CH_2-1), 2.99 (2H, m, CH_2-5), 2.55 (2H, m, CH_2-2), 1.80−1.30 (4H, m, CH_2-3 and CH_2-4); IR (PE) 3600−3000 ($3NH_2$ + 4NH), 1642 (CO), 1627 (2CO), 1112 (COMe); MS *m*/*z* = 585.3 (M^+). Anal. ($C_{31}H_{37}N_8O_4Cl$) Calcd: C 59.97, H 6.01, N 18.06. Found: C 60.35, H 6.08, N 17.79. HPLC (HP) 288 nm, elution by gradient CH_3CN/H_2O (1% TFA) (20:80 to 100:0) for 30 min, t_R = 13.92 min.

Compound 18: ^{1}H NMR (D_2O) δ 8.59 (2H, m, H-3 and H-4), 8.07 (1H, d, H-3′, *J* = 7.5 Hz), 7.78 (4H, m, H-1′, H-2′, H-4′ and H-5), 7.51 (2H, m, H-1 and H-2), 6.73 (1H, s, H-6), 4.28 (1H, m, CH), 4.14 (3H, s, CH_3-N^+), 3.66 (2H, m, CH_2-1), 2.88 (2H, m, CH_2-5), 2.61 (2H, m, CH_2-2), 1.80−1.45 (4H, m, CH_2-3 and CH_2-4); IR (PE) 3600−2600 (OH + $3NH_2$ + 4NH), 1697 (CO), 1625 (2CO); MS *m*/*z* = 571.3 (M^+). Anal. ($C_{30}H_{35}N_8O_4Cl$) Calcd: C 59.38, H 5.82, N 18.48. Found: C 59.21, H 5.78, N 18.79. HPLC (HP) 288 nm, elution by gradient CH_3CN/H_2O (1% TFA) (20:80 to 100:0) for 30 min, t_R = 9.06 min.

Compound 21: ^{1}H NMR (DMSO-d_6) δ 9.00−7.00 (15H, m, $H_{aromatic}$, NHa, NHb, NHc, NHd and NH_2e), 6.80 (2H, bs, $NH_2\alpha$), 6.50 (1H, s, H-6), 6.32 (1H, s, NHβ-$COCF_3$), 4.26 (1H, m, CH), 4.14 (3H, s, CH_3-N^+), 3.58 (3H, s, OMe), 3.48 (2H, m, CH_2-1), 3.09 (2H, m, CH_2-5), 2.51 (2H, m, CH_2-2), 1.80−1.35 (4H, m, CH_2-3 and CH_2-4); MS *m*/*z* = 681.3 (M^+). Anal. ($C_{33}H_{36}N_8O_5F_3Cl$) Calcd: C 55.29, H 5.07, N 15.64. Found: C 55.87, H 5.05, N 16.02. HPLC (HP) 288 nm, elution by gradient CH_3CN/H_2O (1% TFA) (20:80 to 100:0) for 30 min, t_R = 25.91 min.

9-[3-[[(Arginine methyl ester)aminocaproyl]keto]phenyl]-2,7-diamino-10-methylphenanthridine Chloride (16) and 9-[3-[[(Argininyl)aminocaproyl]keto]phenyl]-2,7-diamino-10-methylphenanthridine Chloride (19). This was prepared from **13** (195 mg, 0.21 mmol) by a method analogous to that for **15** above, and the three compounds: the ester **16**, the acid **19**, and the side product **22** were collected

in 37%, 15%, and 28% yields, respectively, as purple resins for **16** and **22** and an orange resin for **19**.

Compound 16: ^{1}H NMR (D_2O) δ 8.45 (2H, m, H-3 and H-4), 8.04 (1H, m, H-3′), 7.73 (3H, m, H-1′, H-2′ and H-4′), 7.37 (3H, m, H-1, H-2 and H-5), 6.54 (1H, s, H-6), 4.05 (4H, m, CH and CH_3 -N^+), 3.59 (3H, s, OMe), 3.30 (2H, m, CH_2-1), 3.02 (2H, m, CH_2-6), 2.55 (2H, m, CH_2-3), 1.85−1.20 (10H, m, $3CH_2$-2, CH_2-4 and CH_2-5); IR (PE) 3600−3000 ($3NH_2$ + 4NH), 1641 (CO), 1627 (2CO), 1110 (COMe); MS m/z = 627.3 (M^+). Anal. ($C_{34}H_{43}N_8O_4Cl$) Calcd: C 61.60, H 6.54, N 16.91. Found: C 61.43, H 6.49, N 16.93. HPLC (HP) 288 nm, elution by gradient CH_3CN/H_2O (1% TFA) (20:80 to 100:0) for 30 min, t_R = 17.66 min.

Compound 19: ^{1}H NMR (D_2O) δ 8.46 (2H, m, H-3 and H-4), 8.04 (1H, m, H-3′), 7.73 (3H, m, H-1′, H-2′ and H-4′), 7.38 (3H, m, H-1, H-2 and H-5), 6.45 (1H, s, H-6), 4.05 (4H, m, CH and CH_3-N^+), 3.30 (2H, m, CH_2-1), 3.01 (2H, m, CH_2-6), 2.30 (2H, m, CH_2-3), 1.90−1.40 (10H, m, $3CH_2$-2, CH_2-4 and CH_2-5); IR (PE) 3600−2600 (OH + $3NH_2$ + 4NH), 1700 (CO), 1627 (2CO); MS m/z = 613.3 (M^+). Anal. ($C_{33}H_{41}N_8O_4Cl$) Calcd: C 61.08, H 6.32, N 17.27. Found: C 61.32, H 6.39, N 17.58. HPLC (HP) 288 nm, elution by gradient CH_3CN/H_2O (1% TFA) (20:80 to 100:0) for 30 min, t_R = 12.79 min.

Compound 22: ^{1}H NMR (DMSO-d_6) δ 9.00−7.00 (15H, m, $H_{aromatic}$, NHa, NHb, NHc, NHd and NH_2e), 6.77 (2H, bs, $NH_2\alpha$), 6.43 (1H, s, H-6), 6.32 (1H, s, NHβ-$COCF_3$), 4.16 (4H, m, CH and CH_3-N^+), 3.60 (3H, s; OMe), 3.28 (2H, m, CH_2-1), 3.02 (2H, m, CH_2-6), 2.30 (2H, m, CH_2-3), 1.85−1.25 (10H, m, $3CH_2$-2, CH_2-4 and CH_2-5); MS m/z = 723.6 (M^+). Anal. ($C_{36}H_{42}N_8O_5F_3Cl$) Calcd: C 59.72, H 5.85, N 15.49. Found: C 60.08, H 5.89, N 15.77. HPLC (HP) 288 nm, elution by gradient CH_3CN/H_2O (1% TFA) (20:80 to 100:0) for 30 min, t_R = 28.83 min.

9-[3-[[[(Arginine methyl ester)-β-alanyl]aminocaproyl]-keto]phenyl]-2,7-diamino-10-methylphenanthridine Chloride (17) and 9-[3-[[(Argininyl-β-alanyl)aminocaproyl]-keto]phenyl]-2,7-diamino-10-methylphenanthridine Chloride (20). This was prepared from **14** (120 mg, 0.12 mmol) by a method analogous to that for **15** above, and the three pure compounds: the ester **17**, the acid **20**, and the side product **23** were isolated in 39%, 23%, and 24% yields, respectively, as purple resins for **17** and **23** and an orange resin for **20**.

Compound 17: ^{1}H NMR (D_2O) δ 8.39 (2H, m, H-3 and H-4), 8.04 (1H, d, H-3′, J = 7.6 Hz), 7.77 (2H, m, H-2′ and H-4′), 7.64 (1H, m, H-1′), 7.37 (3H, m, H-1, H-2 and H-5), 6.55 (1H, s, H-6), 4.18 (1H, m, CH), 4.05 (3H, m, CH_3-N^+), 3.65 (5H, m, OMe and CH_2-1), 3.30 (2H, m, CH_2-4), 3.14 (2H, m, CH_2-8), 2.34 (2H, m, CH_2-5), 2.18 (2H, m, CH_2-3), 1.90−1.35 (10H, m, $3CH_2$-2, CH_2-6 and CH_2-7); IR (PE) 3600−3000 ($3NH_2$ + 5NH), 1642 (CO), 1628 (3CO), 1109 (COMe); MS m/z = 698.4 (M^+). Anal. ($C_{37}H_{48}N_9O_5Cl$) Calcd: C 60.54, H 6.60, N 17.19. Found: C 60.32, H 6.65, N 17.51. HPLC (HP) 288 nm, elution by gradient CH_3CN/H_2O (1% TFA) (20:80 to 100:0) for 30 min, t_R = 16.98 min.

Compound 20: ^{1}H NMR (D_2O) δ 8.38 (2H, m, H-3 and H-4), 8.04 (1H, d, H-3′, J = 7.6 Hz), 7.78 (2H, m, H-2′ and H-4′), 7.64 (1H, m, H-1′), 7.37 (3H, m, H-1, H-2 and H-5), 6.52 (1H, s, H-6), 4.18 (1H, m, CH), 4.05 (3H, m, CH_3-N^+), 3.65 (5H, m, OMe and CH_2-1), 3.30 (2H, m, CH_2-4), 3.14 (2H, m, CH_2-8), 2.34 (2H, m, CH_2-5), 2.18 (2H, m, CH_2-3), 1.90−1.35 (10H, m, $3CH_2$-2, CH_2-6 and CH_2-7); IR (PE) 3600−2600 (OH + $3NH_2$ + 4NH), 1700 (CO), 1627 (3CO); MS m/z = 684.4 (M^+). Anal. ($C_{36}H_{46}N_9O_5Cl$) Calcd: C 60.06, H 6.44, N 17.52. Found: C 60.24, H 6.39, N 17.27. HPLC (HP) 288 nm, elution by gradient CH_3CN/H_2O (1% TFA) (20:80 to 100:0) for 30 min, t_R = 13.36 min.

Compound 23: ^{1}H NMR (DMSO-d_6) δ 9.00−7.00 (16H, m, $H_{aromatic}$, NHa, NHb, NHc, NHd, NHe and NH_2f), 6.75 (2H, bs, $NH_2\alpha$), 6.42 (1H, s, H-6), 6.35 (1H, s, NHβ-$COCF_3$), 4.16 (1H, m, CH), 4.05 (3H, m, CH_3-N^+), 3.65 (5H, m, OMe and CH_2-1), 3.30 (2H, m, CH_2-4), 3.14 (2H, m, CH_2-8), 2.34 (2H, m, CH_2-5), 2.18 (2H, m, CH_2-3), 1.90−1.30 (10H, m, $3CH_2$-2, CH_2-6 and CH_2-7); MS m/z = 794.5 (M^+). Anal. ($C_{39}H_{47}N_9O_6F_3Cl$) Calcd: C 58.92, H 5.96, N 15.87. Found: C 58.63, H 6.00, N 16.07. HPLC (HP) 288 nm, elution by gradient CH_3CN/H_2O (1% TFA) (20:80 to 100:0) for 30 min, t_R = 27.63 min.

***N*-α-[*N*-Benzyloxycarbonyl)-β-alanyl]-*N*-(2,2,5,7,8-pentamethylchroman-6-sulfonyl)arginine (24).** *N*-(Benzyloxycarbonyl)-β-alanine (460 mg, 2.06 mmol) and *N*-hydroxysuccinimide (335 mg, 3.09 mmol) were dissolved in DMF with stirring, at 0 °C. After 15 min, 1,3-dicyclohexylcarbodiimide (425 mg, 2.06 mmol) was added. The reaction mixture was stirred at room temperature for 12 h; then, at 0 °C, H-Arg(Pmc)OH (1 g, 2.27 mmol) was added. The solution was stirred for 12 additional hours, at room temperature, and DMF was removed under reduced pressure. The residue was dissolved in 10% $NaHCO_3$ aqueous solution and then washed with ethyl acetate. The basic aqueous solution was acidified with citric acid (to pH 3), and the product was extracted with ethyl acetate. Organic layers were pooled, washed with water, then dried on $MgSO_4$, and concentrated under reduced pressure. Compound **24** was isolated as a colorless resin (92% yield). This product was used without further purification: TLC (AcOEt/MeOH, 7:3) R_f = 0.30; ^{1}H NMR ($CDCl_3$) δ 7.25 (5H, Ph(Z), s), 6.80 (1H, d, NHb, J = 2.0 Hz), 6.20 (3H, bs, NHc, NHd and NHe), 5.50 (1H, bs, NHa), 5.00 (2H, s, CH_2(Z)), 4.45 (1H, m, CH), 3.35 (2H, m, CH_2-1), 3.10 (2H, m, CH_2-5), 2.60−2.45 (8H, m, $2CH_3$(o) and CH_2-2), 2.35 (2H, m, $CH_2\beta$), 2.00 (3H, s, CH_3(m)), 1.80−1.35 (6H, m, CH_2-3, CH_2-4 and $CH_2\alpha$), 1.25 (6H, m, $2CH_3$gem).

***N*-α-[*N*-(Benzyloxycarbonyl)-β-alanyl]-*N*-(2,2,5,7,8-pentamethylchroman-6-sulfonyl)arginine Methyl Ester (25).** **24** (1.38 g, 2.14 mmol) and cesium carbonate (697 mg, 2.14 mmol) were dissolved in DMF (40 mL). After stirring at room temperature for 10 min, methyl iodide (0.15 mL, 2.35 mmol) was added and stirring was continued for 12 additional hours. DMF was removed under reduced pressure, the residue was dissolved in 10% Na_2CO_3 aqueous solution, and the product was extracted with ethyl acetate. Organic layers were pooled, washed with NaCl aqueous solution, then dried on $MgSO_4$, and concentrated under reduced pressure. The product was purified by chromatography on a silica gel column, with elution by 100% ethyl acetate. After trituration with anhydrous diethyl ether, white crystals of **25** were obtained (56% yield). This product was used without further purification: TLC (AcOEt, 100%) R_f = 0.22; mp = 175−177 °C; ^{1}H NMR ($CDCl_3$) δ 7.25 (5H, s, Ph(Z)), 6.80 (1H, d, NHb, J = 2.0 Hz), 6.20 (3H, bs, NHc, NHd, NHe), 5.50 (1H, bs, NHa), 5.00 (2H, s, CH_2(Z)), 4.45 (1H, m, CH), 3.65 (3H, s, OMe), 3.35 (2H, m, CH_2-1), 3.10 (2H, m, CH_2-5), 2.60−2.45 (8H, m, $2CH_3$(o) and CH_2-2), 2.35 (2H, m, $CH_2\beta$), 2.00 (3H, s, CH_3(m)), 1.80−1.35 (6H, m, CH_2-3, CH_2-4 and $CH_2\alpha$), 1.25 (6H, m, $2CH_3$gem).

***N*-α-[*N*-(Benzyloxycarbonyl)aminocaproyl]-*N*-(2,2,5,7,8-pentamethylchroman-6-sulfonyl)arginine (26).** This was prepared from *N*-(benzyloxycarbonyl)aminocaproic acid (2 g, 7.54 mmol) by a method analogous to that for **24**, and compound **26** was isolated as a white resin (70% yield). This product was used without further purification: TLC (AcOEt/MeOH, 7:3) R_f = 0.22; ^{1}H NMR ($CDCl_3$) δ 7.30 (5H, s, Ph(Z)), 6.20 (1H, d, NHb, J = 2.0 Hz), 6.00 (3H, bs, NHc, NHd and NHe), 5.0 (3H, m, NHa and CH_2(Z)), 4.50 (1H, m, CH), 3.15 (4H, m, CH_2-1 and CH_2-6), 2.50 (10H, m, CH_2-3, $2CH_3$(o) and $CH_2\beta$), 2.30 (2H, m, $CH_2\alpha$), 2.05 (3H, s, CH_3(m)), 1.70 (6H, m, $3CH_2$-2), 1.60 (4H, m, CH_2-4 and CH_2-5), 1.30 (6H, m, $2CH_3$gem).

***N*-α-[*N*-(Benzyloxycarbonyl)aminocaproyl]-*N*-(2,2,5,7,8-pentamethylchroman-6-sulfonyl)arginine Methyl Ester (27).** This was prepared from **26** (345 mg, 0.50 mmol) by a method analogous to that for **25**, except the chromatography column eluant was now 10% methanol in ethyl acetate. Compound **27** was obtained as white crystals (55% yield). This product was used without further purification: TLC (AcOEt, 100%) R_f = 0.42; mp = 140−142 °C; ^{1}H NMR ($CDCl_3$) δ 7.30 (5H, s, Ph(Z)), 6.20 (1H, d, NHb, J = 2.0 Hz), 6.00 (3H, bs, NHc, NHd and NHe), 5.0 (3H, m, NHa and CH_2(Z)), 4.50 (1H, m, CH), 3.70 (3H, s, OMe), 3.15 (4H, m, CH_2-1 and CH_2-6), 2.50 (10H, m, CH_2-3, $2CH_3$(o) and $CH_2\beta$), 2.30 (2H, m, $CH_2\alpha$),

2.05 (3H, s, CH_3(m)), 1.70 (6H, m, $3CH_2$-2), 1.60 (4H, m, CH_2-4 and CH_2-5), 1.30 (6H, m, $2CH_3$gem).

***N*-α-[[*N*-(Benzyloxycarbonyl)aminocaproyl]-*β*-alanyl]-*N*-(2,2,5,7,8-pentamethylchroman-6-sulfonyl)arginine Methyl Ester (28).** *N*-(Benzyloxycarbonyl)aminocaproic acid (288 mg, 1.09 mmol), 1-hydroxybenzotriazole (142 mg, 1.31 mmol), **9** (572 mg, 1.09 mmol), and 1,3-dicyclohexylcarbodiimide (225 mg, 1.09 mmol) were dissolved in DMF (30 mL), at 0 °C. The reaction mixture was stirred, at room temperature, for 18 h. The DCU precipitate was filtered and DMF removed under reduced pressure. The residue was dissolved in ethyl acetate. Organic layer was washed with 10% $NaHCO_3$ aqueous solution, then with 10% citric acid aqueous solution, and with water, finally dried on $MgSO_4$, and concentrated under reduced pressure. The product was purified by chromatography on a silica gel column, with elution by 10% methanol in ethyl acetate, and compound **28** was isolated as a colorless oil (70% yield). This product was used without further purification: TLC (AcOEt, 100%) $R_f = 0.21$; ^{1}H NMR ($CDCl_3$) δ 7.30 (5H, s, Ph(Z)), 6.20 (2H, m, NHb and NHc), 6.00 (3H, bs, NHd, NHe and NHf), 5.0 (3H, m, NHa and CH_2(Z)), 4.50 (1H, m, CH), 3.70 (3H, s, OMe), 3.35 (2H, m, CH_2-8), 3.15 (4H, m, CH_2-1 and CH_2-4), 2.50 (12H, m, CH_2-3, CH_2-5, $2CH_3$(o) and $CH_2\beta$), 2.30 (2H, m, $CH_2\alpha$), 2.05 (3H, s, CH_3(m)), 1.60 (4H, m, CH_2-6 and CH_2-7), 1.50 (6H, m, $3CH_2$-2), 1.30 (6H, m, $2CH_3$gem).

Cells and Viruses. CEM-SS and MT4 cells were cultured in RPMI medium supplemented with 10% fetal calf serum (heated at 56 °C for 30 min). CEM-SS cells were obtained from Peter Nara through AIDS Research and Reference Reagent Program, Division of AIDS, NIAd, NIH. HIV-1 LAI and HIV IIIB were produced in CEM-SS cells as previously reported.[59]

Anti-HIV-1 Activity and Cytotoxicity Measurements in Vitro on CEM-SS Infected and Uninfected Cells. The effect of the compounds on the replication of HIV-1 LAI in acutely infected CEM-SS cells was evaluated using a procedure previously described[59] with slight modifications. The rate of virus production was measured by quantification of the reverse transcriptase activity associated with the virus particles released in the culture supernatant. Briefly, cells were infected with $TCID_{50}$; after a 30-min adsorption period, unbound particles were removed and cells were cultured in the presence of different concentrations of tested compounds for 5 days before determining rates of virus production. Three measurements were carried out for each concentration of each compound. The 50% inhibitory concentration of virus replication (IC_{50}) was derived from the computer-generated median plot of the dose−effect data.[60] The cytotoxicity of the molecules for uninfected cells was measured after an incubation of 5 days in the presence of various drug concentrations, using a colorimetric assay (MTT test).[61] Again, three measurements were carried out for each concentration of each compound. The 50% cytotoxicity concentration (CC_{50}) at which OD_{540} was reduced by one-half was calculated using the program mentioned above. The entire experiment was repeated twice.

Anti-HIV-1 Activity and Cytotoxicity Measurements in Vitro on MT4 Infected and Uninfected Cells. The anti-HIV-1 test based on MT4 infected cells was previously described.[62,63] Measurements were performed in triplicate for each concentration of each compound, and the entire experiment was repeated twice. Briefly, in MT4 cells, the determination of the antiviral activity of the tested compounds was based on a reduction of HIV-1-induced pathogenicity, the metabolic activity of the cells being measured by the ability of mitochondrial dehydrogenases to reduce 3-(4,5-dimethylthiazol-2-yl)-2,5-diphenyltetrazolium bromide (MTT) to formazan. When the inhibition did not reach 50%, the measured value is indicated in parentheses.

Anti-HIV-1 Activity and Cytotoxicity Measurements in Vitro on PBMC Infected and Uninfected Cells. The techniques used for measuring inhibition of virus multiplication were previously described.[59−61] Measurements were performed in triplicate for each concentration of each compound, and the entire experiment was repeated twice. Briefly, PBMC cells were cultured in the presence of different concentrations of tested compounds for 7 days, after virus incubation in cell cultures. The production of virus HIV-1 was measured by quantification of the reverse transcriptase activity in the culture supernatant. Cytotoxicity of the drugs was measured after incubation for 7 days in their presence using the colorimetric MTT test. When the inhibition did not reach 50%, the measured value is indicated in parentheses.

Dynamic Molecular Modeling Studies. The three-dimensional structures of (i) Tat protein−TAR RNA complex, (ii) free TAR RNA, and (iii) TAR RNA with an arginine residue were found in the Protein Data Bank. All molecular modeling studies except the arginine−TAR RNA approach were performed using the Insight II molecular modeling package. Energy was computed with Cff91 as force field, and minimization was performed using the conjugate gradient algorithm with 9000 iteration steps or until convergence (defined as an energy gradient of 0.0001 kcal/mol or less). The geometric constraints were created with the specific command "genericdist" of the discover module. The annealing was defined by 50 cycles of 3000 minimization steps followed by 5000 steps of molecular dynamic with a temperature of 300 K. For the arginine−TAR RNA approach, the Sybyl package was used. Interaction energy was calculated by the MM2 force field and minimization performed using the conjugate gradient algorithm with 5000 iteration steps. Visualization of different interactions between arginine and TAR RNA was made with the Sybyl program and all others with the Insight II program. All calculations were done on a IRIS indigo 2 R10.000 of the Centre de Modélisation et d'Imagerie Moléculaire of UNSA.

In Vitro Transcription. Synthetic oligonucleotides corresponding to the wild-type or the bulge-deleted (ΔU) TAR sequences were cloned between *Hin*dIII and *Eco*RI sites of the pUC19 plasmid. After digestion with *Eco*RI, the RNA was transcribed as a runoff product of 60 nucleotides from the T3 RNA polymerase promoter. In each case the transcript included an additional G residue on the 3′-end derived from the *Eco*RI cleavage site. Transcription reaction was performed in buffer containing 40 mM Tris-HCl, pH 7.4, 25 mM NaCl, 16 mM $MgCl_2$, 10 mM DTT, and 1 mM NTPs. The reaction was initiated by addition of 10 μg linearized plasmid DNA template and 40 units T3 RNA polymerase and incubated for 2 h at 37 °C. Nucleic acids were then fractionated on a 10% (w/v) polyacrylamide gel containing 8 M urea in TBE buffer (89 mM Tris-borate, pH 8.3, 10 mM EDTA). After electrophoresis, the RNA was eluted in water for 18 h at 4 °C and precipitated with ethanol. The RNA was resuspended in water to give a 500 μM stock solution (ϵ^{260}/phosphate = 10 688 M^{-1} cm^{-1}). For the footprinting experiments, the RNA was 3′-end labeled with [^{32}P]cytidine biphosphate and T4 RNA ligase and then purified again from a 10% denaturing acrylamide gel. RNA solutions were prepared with doubly distilled sterile water to prevent from nuclease contamination. Tubes and tips were treated with 1% diethyl pyrocarbonate (DEPC from Sigma).

Melting Temperature Studies. Absorption spectra were recorded on a Uvikon 943 spectrophotometer. The 12-cell holder was thermostated with a Neslab RTE 111 cryostat. Drug−RNA complexes were prepared by adding aliquots of a concentrated CGP40336A solution to a RNA solution at constant concentration (usually 20 μM) in BPE buffer, pH 7.1 (6 mM Na_2HPO_4, 2 mM $Na_2H_2PO_4$, 1 mM EDTA). A heating rate of 1 °C/min was used, and data points were collected every 30 s. The temperature inside the cuvette was monitored by using a thermocouple. The absorbency at 260 nm was measured over the range 25−90 °C in 1-cm path length reduced volume quartz cells. The "melting" temperature T_m was taken as the midpoint of the hyperchromic transition determined from first-derivative plots. The reproducibility of the T_m measurements was ±0.5 °C.

RNase Footprinting. Samples of the labeled RNA fragment were incubated with a buffered solution containing the desired drug concentration. After 20-min incubation at 4 °C to ensure equilibration, the digestion was initiated by addition of the RNase (A, T1, or V1) solution. The RNases (Pharmacia

Biotech, Saclay, France) were used according to the supplier's recommended protocol in the activity buffer provided. After 1-min incubation at room temperature, the reaction was stopped by freeze-drying and samples were lyophilized. The RNA in each tube was resuspended in 5 μL of formamide-TBE loading buffer, denatured at 90 °C for 4 min, and then chilled in ice for 4 min prior to loading on to a 0.3-mm thick, 10% polyacrylamide gel containing 8 M urea and TBE buffer (89 mM Tris base, 89 mM boric acid, 2.5 mM Na_2EDTA, pH 8.3). After 2-h electrophoresis at 1500 V, the gel was soaked in 10% acetic acid for 10 min, transferred to Whatman 3MM paper, dried under vacuum at 80 °C, and then analyzed on the Phosphorimager (Molecular Dynamics). Each resolved band on the autoradiograph was assigned to a particular bond within the RNA fragment by comparison of its position relative to sequencing standards generated by treatment of the RNA with diethyl pyrocarbonate followed by aniline-induced cleavage at the modified bases (A track).

Acknowledgment. We are grateful to J. M. Guigonis for doing the mass spectrometry analyses. We express our warmest thanks to Dr. R. A. Earl for reading the manuscript and for helpful suggestions. Thanks are also due to Dr. T. T. Tran for helpful discussions and suggestions. This work was supported by grants from ANRS (Agence Nationale de Recherches sur le SIDA) and SIDACTION (Fondation pour la Recherche Médicale).

References

(1) Barré-Sinoussi, F.; Chermann, J. C.; Rey, F.; Nugeyre, M.; Chamaret, S.; Gruest, J.; Dauguet, C.; Axler-Blin, C.; Vezinet-Brun, F.; Rouzioux, C.; Rozenbaum, W.; Montagnier, L. Isolation of a T-lymphotropic retrovirus from a patient at risk of acquired immune deficiency syndrome (AIDS). *Science* **1983**, 868−870.

(2) Kingsman, S. M.; Kingsman, A. J. The regulation of human immunodeficiency virus type-1 gene expression. *Eur. J. Biochem.* **1996**, 491−507.

(3) Caputo, A.; Grossi, M. P.; Rossi, C.; Campioni, D.; Balboni, P. G.; Corallini, A.; Barbanti-Brodano, G. The *tat* gene and protein of the human immunodeficiency virus type 1. *Microbiologica* **1995**, 87−110.

(4) Felber, B. K.; Pavlakis, G. N. Molecular biology of HIV-1-positive and negative regulatory elements important for virus expression. *AIDS* **1993**, S51−S62.

(5) Marciniak, R. A.; Sharp, P. A. HIV-1 Tat protein promotes formation of non processive elongation complexes. *EMBO J.* **1991**, 4189−4196.

(6) Bayer, P.; Kraft, M.; Ejchart, A.; Westendorp, M.; Frank, R.; Rosch, P. Structural studies of HIV-1 Tat protein. *J. Mol. Biol.* **1995**, 529−535.

(7) Vives, E.; Charneau, P.; Van Rietschoten, J.; Rochat, H.; Bahraoui, E. Effects of the Tat basic domain on human immunodeficiency virus type 1 *trans*-activation, using chemically synthesized Tat protein and Tat peptides. *J. Virol.* **1994**, 3343−3353.

(8) Karn, J.; Graeble, M. A. New insights into the mechanism of HIV-1 *trans*-activation. *Trends Genet.* **1992**, 365−368.

(9) Tao, J.; Frankel, A. D. Electrostatic interactions modulate the RNA-binding and *trans*-activation specificities of the HIV and SIV Tat proteins. *Proc. Natl. Acad. Sci. U.S.A.* **1993**, 1571−1575.

(10) Churcher, M. J.; Lamont, C.; Hamy, F.; Dingwall, C.; Green, S. M.; Lowe, A. D.; Butler, P. J. G.; Gait, M. J.; Karn, J. High affinity binding of TAR RNA by the human immunodeficiency virus Type-1 Tat protein requires base-pairs in the RNA stem and amino acid residues flanking the basic region. *J. Mol. Biol.* **1993**, 90−110.

(11) Weeks, K.; Crothers, D. M. RNA recognition by Tat-derived peptides: interaction in the major groove. *Cell* **1991**, 577−588.

(12) Jones, K. A.; Peterlin, B. M. Control of RNA initiation and elongation at the HIV-1 promoter. *Annu. Rev. Biochem.* **1994**, 717−743.

(13) Cullen, B. R. Mechanism of action of regulatory proteins encoded by complex retroviruses. *Microbiol. Rev.* **1993**, 375−394.

(14) Muesing, M. A.; Smith, D. H.; Capon, D. J. Regulation of mRNA accumulation by HIV *trans*-activation protein. *Cell* **1987**, 691−704.

(15) Aboul-Ela, G.; Karn, J.; Varani, G. Structure of HIV-1 TAR RNA in the absence of ligands reveals a novel conformation of the trinucleotide bulge. *Nucleic Acids Res.* **1996**, 4598−4598.

(16) Wang, Z. Y.; Rana, T. M. RNA conformation in the Tat-TAR complex determined by site-specific photocross-linking. *Biochemistry* **1996**, *35*, 6491−6499.

(17) Aboul-Ela, F.; Karn, J.; Varani, G. The structure of the human immunodeficiency virus type-1 TAR RNA reveals principles of RNA recognition by Tat protein. *J. Mol. Biol.* **1995**, *253*, 313−332.

(18) Sumner-Smith, M.; Roy, S.; Barnett, R.; Reid, L. S.; Kuperman, R.; Delling, U.; Sonenberg, N. Critical chemical features in *trans*-acting-responsive RNA are required for interaction of HIV-1 Tat protein. *J. Virol.* **1991**, 5196−5202.

(19) Pritchard, C. E.; Grasby, J. A.; Hamy, F.; Zacharek, A. M.; Singh, M.; Karn, J.; Gait, M. J. Methylphosphonate mapping of phosphate contacts critical for RNA recognition by the human immunodeficiency virus tat and rev proteins. *Nucleic Acids Res.* **1994**, 2592−2600.

(20) Hamy, F.; Asseline, U.; Grasby, J.; Iwai, S.; Pritchard, C.; Slim, G.; Butler, P. J. G.; Karn, J.; Gait, M. J. Hydrogen-bonding contacts in the major groove are required for human immunodeficiency virus type-1 Tat protein recognition of TAR RNA. *J. Mol. Biol.* **1993**, 111−123.

(21) Calnan, B. J.; Tidor, B.; Biancalana, S.; Hudson, D.; Frankel, A. D. Arginine-mediated RNA recognition: the arginine fork. *Science* **1991**, 1167−1171.

(22) Delling, U.; Roy, S.; Sumner-Smith, M.; Barnett, R.; Reid, L.; Rosen, C. A.; Sonenberg, N. The number of positively charged amino acids in the basic domain of Tat is critical for *trans*-activation and complex formation with TAR RNA. *Proc. Natl. Acad. Sci. U.S.A.* **1991**, 6234−6238.

(23) Tao, J.; Chen, L.; Frankel, A. D. Dissection of the proposed base triple in HIV TAR RNA indicates the importance of the Hoogsteen interaction. *Biochemistry* **1997**, 3491−3495.

(24) Puglisi, J. D.; Tan, R.; Calnan, B. J.; Frankel, A. D.; Williamson, J. R. Conformation of the TAR-arginine complex by NMR. *Science* **1992**, 76−80.

(25) Puglisi, J. D.; Chen, L.; Frankel, A. D.; Williamson, J. R. Role of RNA structure in arginine recognition of TAR RNA. *Proc. Natl. Acad. Sci. U.S.A.* **1993**, 3680−3684.

(26) Tao, J.; Frankel, A. D. Specific binding of arginine to TAR RNA. *Proc. Natl. Acad. Sci. U.S.A.* **1992**, 2723−2726.

(27) Wilson, W. D.; Ratmeyer, L.; Zhao, M.; Strekowski, L.; Boykin, D. The search for structure-specific nucleic acid-interactive drugs: effects of compound structure on RNA versus DNA interaction strength. *Biochemistry* **1993**, *32*, 4098−4104.

(28) Jain, S. C.; Sobell, H. M. Visualization of drug-nucleic acid interactions at atomic resolution. VIII. Structures of two ethidium/dinucleoside monophosphate crystalline complexes containing ethidium: cytidylyl(3′-5′)guanosine. *J. Biomol. Struct. Dyn.* **1984**, 1179−1194.

(29) Kastrup, R. V.; Young, M. A.; Krugh, T. R. Ethidium bromide complexes with self-complementary deoxytetranucleotides. Demonstration and discussion of sequence preferences in the intercalative binding of ethidium bromide. *Biochemistry* **1978**, *17*, 485−4865.

(30) Krugh, T. R.; Reinhardt, C. G. Evidence for sequence preferences in the intercalative binding of ethidium bromide to dinucleoside monophosphates. *J. Mol. Biol.* **1975**, 133−162.

(31) Fox, K. R.; Waring, M. J. Footprinting at low temperature: evidence that ethidium and other simple intercalators can discriminate between different nucleotide sequences. *Nucleic Acids Res.* **1987**, 491−507.

(32) White, S. A.; Draper, D. E. Single base bulges in small RNA hairpins enhance binding and promote an allosteric transition. *Nucleic Acid Res.* **1987**, 4049−4064.

(33) White, S. A.; Draper, D. E. Effects of single-base bulges on intercalator binding to small RNA and DNA hairpins and a ribosomal RNA fragment. *Biochemistry* **1989**, *28*, 1892−1897.

(34) Yao, S.; Wilson, W. D. A molecular mechanics investigation of RNA complexes. I. Ethidium intercalation in an HIV-1 TAR RNA sequence with an unpaired adenosine. *J. Biomol. Struct. Dyn.* **1992**, 367−387.

(35) Ratmeyer, L. S.; Vinayak, R.; Zon, G.; Wilson, W. D. An ethidium analogue that binds with high specificity to a base-bulged duplex from the TAR RNA region of the HIV-1 genome. *J. Med. Chem.* **1992**, *35*, 966−968.

(36) Veal, J. M.; Wilson, W. D. Modeling of nucleic acid complexes with cationic ligands: a specialized molecular mechanics force field and its application. *J. Biomol. Struct. Dyn.* **1991**, 1119−1145.

(37) Mei, H.-Y.; Cui, M.; Heldsinger, A.; Lemrow, S. M.; Loo, J. A.; Sannes-Lowery, K. A.; Sharmeen, L.; Czarnik, A. W. Inhibitors of protein-RNA complexation that target the RNA: Specific recognition of human immunodeficiency virus type 1 TAR RNA by small organic molecules. *Biochemistry* **1998**, *14204*, 14204−14212.

(38) Hamy, F.; Felder, E. R.; Heizmann, G.; Lazdins, J.; Aboul-Ela, F.; Varani, G.; Karn, J.; Klimkait, T. An inhibitor of the Tat/TAR RNA interaction that effectively suppresses HIV-1 replication. *Proc. Natl. Acad. Sci. U.S.A.* **1997**, 3548−3553.
(39) Chen, Q.; Shafer, R. H.; Kuntz, I. D. Structure-based discovery of ligands targeted to the RNA double helix. *Biochemistry* **1997**, 11402−11407.
(40) Pearson, N. D.; Prescott, C. D. RNA as a drug target. *Chem. Biol.* **1997**, 409−414.
(41) Mei, H. Y.; Mack, D. P.; Galan, A. A.; Halim, N. S.; Heldsinger, A.; Loo, J. A.; Moreland D. W.; Sannes-Lowery, K. A.; Sharmeen, L.; Truong, H. N.; Czarnik, A. W. Discovery of selective, small-molecule inhibitors of RNA complexes − I. The Tat protein/TAR RNA complexes required for HIV-1 transcription. *Bioorg. Med. Chem.* **1997**, 1173−1184.
(42) Kurz, K.; Gobel, M. W. Hydrolytical cleavage of TAR RNA, the *trans*-activation responsive region of HIV-1, by a bis(guanidinium) catalyst attached to arginine. *Helv. Chim. Acta* **1996**, 1967−1979.
(43) Wilson, W. D.; Tanious, F. A.; Fernandez-Saiz, M.; Rigl, C. T. Evaluation of drug-nucleic acid interactions by thermal melting curves. *Methods Mol. Biol.* **1997**, 219−240.
(44) Lapidot, A.; Ben-Asher, E.; Eisenstein, M. Tetrahydropyrimidine derivatives inhibit binding of a Tat-like, arginine-containing peptide, to HIV TAR RNA in vitro. *FEBS Lett.* **1995**, 33−38.
(45) Michne, W. F.; Schroeder, J. D.; Bailey, T. R.; Neumann, H. C.; Cooke, D.; Young, D. C.; Hughes, J. V.; Kingsley, S. D.; Ryan, K. A.; Putz, H. S. Keto/enol epoxy steroids as HIV-1 Tat inhibitors: structure−activity relationships and pharmacophore localization. *J. Med. Chem.* **1995**, *38*, 3197−3206.
(46) Mei, H. Y.; Galan, A. A.; Halim, N. S.; Mack, D. P.; Moreland, D. W.; Sanders, K. B.; Truong, H. N.; Czarnik, A. W. Inhibition of an HIV-1 Tat-derived peptide binding to TAR RNA by aminoglycoside antibiotics. *Bioorg. Med. Chem. Lett.* **1995**, 2755−2760.
(47) Coffen, D. L.; Huang, T. N.; Ramer, S. E.; West, R. C.; Connell, E. V.; Schutt, A. D.; Hsu, M. C. Discovery of a drug lead employing a peptide library − Inhibition of HIV-1 Tat and viral replication by the tripeptide YPG-NH_2. *Antiviral Chem. Chemother.* **1994**, 128−129.
(48) Wilson, W. D.; Ratmeyer, L.; Cegla, M. T.; Spychala, J.; Voykin, D.; Demeunynck, M.; Lhomme, J.; Krishnan, G.; Kennedy, D.; Vinayak, R.; Zon, G. Bulged-base nucleic acids as potential targets for antiviral drug action. *New J. Chem.* **1994**, 419−423.
(49) Sinet, M.; Kubar, J.; Condom, R.; Patino, N.; Guedj, R. The protein Tat of HIV − Potential target in antiretroviral chemotherapy. *Médecine/Sciences* **1993**, 1342−1351.
(50) Kuhlmann, K. F.; Charbeneau, N. J.; Mosher, C. W. Synthesis, DNA-binding and biological activity of a double intercalating analogue of ethidium bromide. *Nucleic Acids Res.* **1978**, 2629−2641.
(51) Konakahura, T.; Wurdeman, R. L.; Gold, B. Synthesis of an *N*-methyl-*N*-nitrosourea linked to a methidium chloride analogue and its reactions with ^{32}P-end-labeled DNA. *Biochemistry* **1988**, 8606−8613.
(52) Lion, C.; Boukou-Poba, J. P.; Charvy, C. Synthèse dans la chimie des phénanthridines. I. Recherches des conditions optimales dans la préparation d′alkyl-6 phénanthridines et de leur sel. *Bull. Soc. Chim. Belg.* **1989**, 557−573.
(53) Lion, C.; Boukou-Poba, J. P.; Charvy, C. Synthèse dans la chimie des phénanthridines. III. Préparation de quelques modèles d′acides *ω*-(diamino-3,8-phénanthridinyl-6) carboxyliques. *Bull. Soc. Chim. Belg.* **1990**, 171−181.
(54) Fodor, G.; Nagubandi, S. Correlation of the Von Braun, Ritter, Bischler-Napieralski, Beckmann and Schmidt reactions via nitrilium salt intermediates. *Tetrahedron* **1980**, 1279−1300.
(55) Ramage, G.; Green, J. N^G-2,2,5,7,8-Pentamethylchroman-6-sulphonyl-L-arginine: a new acid labile derivative for peptide synthesis. *Tetrahedron Lett.* **1987**, 2287−2290.
(56) Ramage, G.; Green, J.; Blake, A. J. An acid labile arginine derivative for peptide synthesis: N^G-2,2,5,7,8-pentamethylchroman-6-sulphonyl-L-arginine. *Tetrahedron Lett.* **1991**, 6353−6370.
(57) Terreux, R.; Peytou, V.; Condom, R.; Cabrol-Bass, D.; Guedj, R. Modeling of interaction between new ethidium derivatives and TAR RNA of HIV-1. *J Chem. Inf. Comput. Sci.* **1999**, 413−419.
(58) It is very unlikely that the drug binds directly to the RNase enzymes for two reasons. First, we used the same concentration of enzyme to cleave the RNA alone and the RNA complexed with the drug. If the ligand was bound to the enzyme, then the level of RNA cleavage would be reduced, but this is not the case. Second, we investigated the binding of the drug to another hairpin RNA related to RRE RNE from HIV-1, but no cleavage protection was detected. For these reasons, we are convinced that the observed effects reflect the interaction of the drug with the RNA and not with the enzyme.
(59) Moog, C.; Wick, A.; Leber, P.; Kirn, A.; Aubertin, A. M. Bicyclic imidazo derivatives, a new class of highly selective inhibitors for the HIV-1. *Antiviral Res.* **1994**, 275−288.
(60) Chou, J.; Chou, T. C. In dose−effect analysis with microcomputers: quantitation of ED_{50}, LD_{50}, synergism, antagonism, low-dose risk, receptor binding and enzyme kinetics. *Computer software for Apple II series and IBM-PC and instruction manual;* Elsevier-Biosoft, Elsevier Science: Cambridge, U.K., 1985.
(61) Mosmann, T. Rapid colorimetric assay for cellular growth and survival: application to proliferation and cytotoxicity assays. *Imunnol. Methods* **1983**, 55−63.
(62) Pauwels, R.; Balzarini, J.; Baba, M.; Snoeck, R.; Schols, D.; Herdewijn, P.; Desmyter, J.; De Clercq, E. Rapid and automated tetrazolium-based colorimetric assay for the detection of anti-HIV compounds. *J. Virol. Methods* **1988**, 309−321.
(63) Génu-Dellac, C.; Gosselin, G.; Puech, F.; Henry, J. C.; Aubertin, A. M.; Aubert, G.; Kirn, A.; Imbach, J. L. Systematic synthesis and antiviral evaluation of α-L-arabinofuranosyl and 2′-deoxy-α-L-erythro-pentufuranosyl nucleosides of the five naturally occurring nucleic acid bases. *Nucleosides Nucleotides* **1991**, 1345−1376.

JM980728E